DEVELOPMENT OF THE DUAL SLOT RESONANCE LINAC*

N. Barov, D. Newsham, X. Chang, R.H. Miller, R. Wu,
FAR-TECH Inc., San Diego, CA 92121, USA

Abstract

We report the status of the Dual Slot Resonance (DSR) linac under development by FAR-TECH. In this linac type, cell-to-cell coupling is provided by a pair of close-coupled resonant slots, resulting in very strong coupling vs. a typical side-coupled linac design, as well as a much more compact radial space requirement. We discuss the status of the structure fabrication, the RF distribution system, and planned installation and testing at the UCLA Pegasus laboratory.

INTRODUCTION

The basic concept of the DSR linac was reported in [1], and that article contains a more in-depth explanation of this linac type. FAR-TECH has applied for patent for this technology [2]. The geometry of a pair of linac cells is shown in Figure 1, which shows a half-geometry of the vacuum region inside the linac structure. A group of two resonant slots connect two adjacent linac cells through an intervening swept triangular volume which we refer to as a "void". The void region serves to provide RF coupling between the two slots. Each group of two slots has two collective resonant modes: a mode at around 1 GHz, and the working mode at 2.856 GHz, our target operating frequency. The mode split between these collective modes is so large that the pair of slots can effectively be considered a single oscillator at 2.856 GHz. The two slots serve the same purpose as a coupling cell in a side coupled linac.

The advantages of the DSR linac are the following:

- Very large coupling with about 24% bandwidth.
- Compact geometry; no additional radial space required for the coupling cells.
- Shunt impedance competitive with a side-coupled linac.

Simulations with HFSS [3] and with Omega3P [4] predict a shunt impedance ZT^2 of 85 MΩ/m. This is competitive with other linac designs featuring large coupling such as the PWT design [5], and is slightly less efficient than an equivalent side-coupled linac, which might have about 8-10% higher ZT^2 with the same basic cavity shape.

The linac will eventually be installed at the UCLA Pegasus laboratory to aid in ultra-short electron bunch experiments [6], where it will be capable of boosting the beam energy by 10 MeV. The linac can also be operated in bunching phase, which will further shorten the bunch length and enable better resolution for experiments such as electron diffraction studies.

It is hoped that the DSR linac design will also find use in medical, industrial, and X-ray inspection applications.

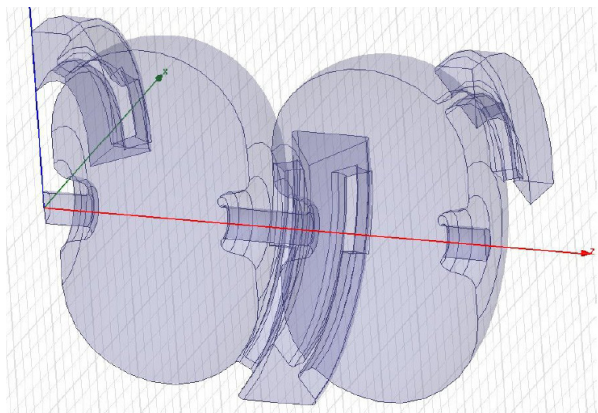

Figure 1: An HFSS model of the RF region half-geometry, showing two linac cells.

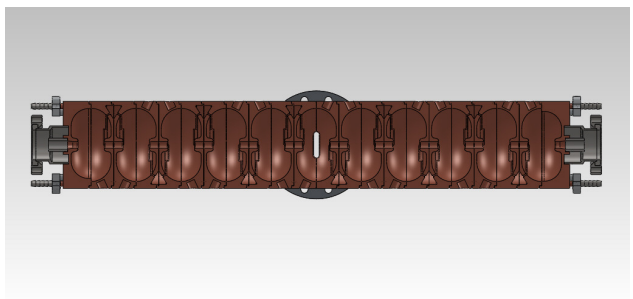

Figure 2: The updated 11-cell linac design.

DESIGN AND FABRICATION

11-Cell Design

The previous design consisted of 10+2/2 cells. We performed RF modeling and component design to change the layout to an 11-cell structure, shown in Figure 2. As with the previous design, the end cells are moved slightly off-axis to minimize the dipole kick. The advantages of the new design include:

- The number of distinct parts was reduced by two.
- The new full cells have larger shunt impedance than half cells.
- Waveguide coupling is now at the middle cell, which is better from a symmetry stand point.
- The structure has two fewer braze joints.
- The structure has two fewer modes within the passband, and hence ~10% larger spacing to nearby modes.

The modification to an 11-cell design was not a difficult change to make, as it did not affect any of the already

*Work supported by DOE Office of High Energy Physics, DOE-SBIR #DE-FG02-08ER85034

ISBN 978-3-95450-115-1

Copyright © 2012 by IEEE – cc Creative Commons Attribution 3.0 (CC BY 3.0) — cc Creative Commons Attribution 3.0 (CC BY 3.0)

designed linac parts except for the end cells, which were re-designed as new parts.

Fabrication and Test Braze

All copper components have been fabricated and are awaiting the brazing step. Due to the geometry of the slots, 5-axis machining was required. Although the programming and setup of the 5-axis machining center is more complicated than for more standard linac parts, once the process has been optimized, the parts can be inexpensively produced. The batch of parts we received had a certain amount of material build-up (built-up edge) and chatter marks, and this needed to be de-burred and polished by hand. Figure 3 shows a finished half-cavity part.

The cavity half shown in Figure 3 has a thin wall section in the half-circular region from the cavity center to the slot. There is some danger that when two cavity half parts are brazed together, that region will sag from the pressure at the braze joint. A test braze was performed using pieces that mechanically resemble the actual components, and the amount of sag was measured with a precision depth gage. The examination did not find any distortion attributable to sag, and we are therefore confident to proceed with brazing the actual linac parts.

Figure 3: A finished half-cavity copper part.

Structure Braze and Final Tuning

The copper components are now ready for the first braze cycle. The braze shims for this operation have also been acquired. In the first braze cycle, sets of two cavity halves are joined together as in the above braze test. After this step, the assemblies will be stacked into several different configurations in order to perform final structure tuning and to make a bead pull analysis (see Figure 5) to check for field imbalance between cells. The components can be stacked in several different ways in order to test different RF properties.

An important condition that should be met in any $\pi/2$ phase advance linac is to achieve a closed dispersion curve. The case where all slots are tuned to a different frequency than all cavities creates a stop band in the dispersion curve, which takes away a major advantage of a $\pi/2$ structure, namely operation on the maximally steep point on the dispersion curve. We have built a simplified time-dependent coupled oscillator model in MATLAB to test the effect of mis-tuning on structure fill time and cell-to-cell field balance, shown in Figure 4. This plot shows an initial time delay of about 20 ns before the power reaches the end cells, and some sloshing with a period of 50 ns between the end cells and the middle cell where power is introduced. This case was also run with a relatively severe mis-tuning of around 40 MHz, according to a semi-random detuning model, which resulted in significant field im-balance. Keeping the slots tuned to within 3 MHz of the operating frequency appears to not have any deleterious effect on the structure mode. This relatively relaxed tuning requirement is a result of the large bandwidth designed into the structure.

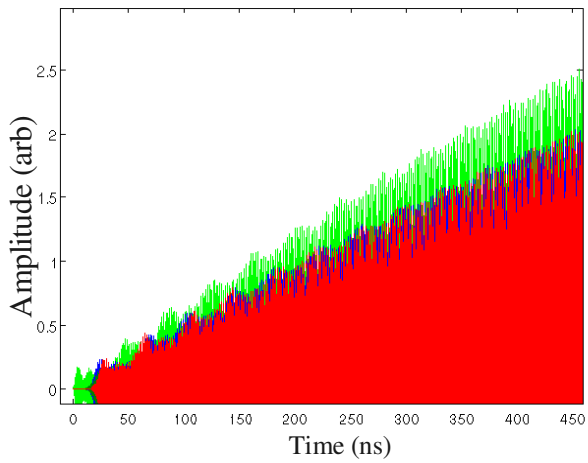

Figure 4: Simple oscillator model to explore effects of improper tuning. Middle cell is shown in green, and end cells are in red and blue.

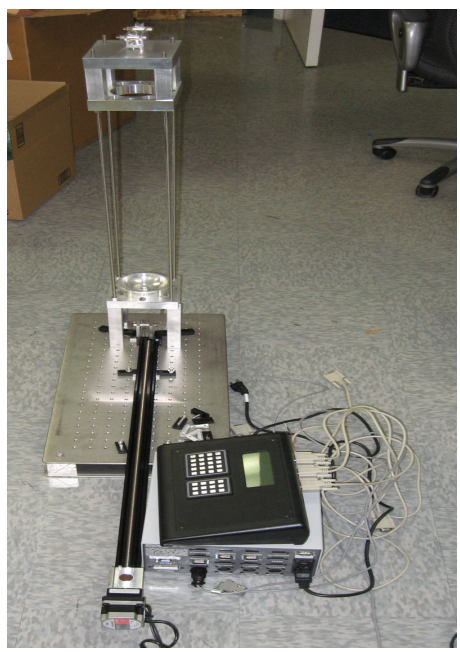

Figure 5: The bead pull fixture and motion control system.

Copyright © 2012 by IEEE – cc Creative Commons Attribution 3.0 (CC BY 3.0) — cc Creative Commons Attribution 3.0 (CC BY 3.0)

The brazed assemblies can be stacked in several ways to test for a closed dispersion curve. First, conducting plane end caps can be placed on the midplane of each cell. The second configuration involves two specially fabricated end caps made from a half cell with a conducting plane brazed half way through the triangular "void" region. The frequency in each test will be tuned to the operating frequency, which achieves the closed dispersion curve condition. Further tests can also be made by incorporating an end cell or a waveguide coupler cell into the stack. Since the end cells maintain the full 8 mm beam aperture, they can be used in the bead pull analysis.

After completing the RF tests, the linac will be sent for the final braze step. Some limited tuning of the operating frequency will be possible after the final braze. Each cell has a dimple tuner, and the end cells have a deformable wall connected to a threaded stainless steel tube that can tune the structure either up or down in frequency (see Figure 1). The final tuning adjustment is through the operating temperature of the structure as set by the water cooling system.

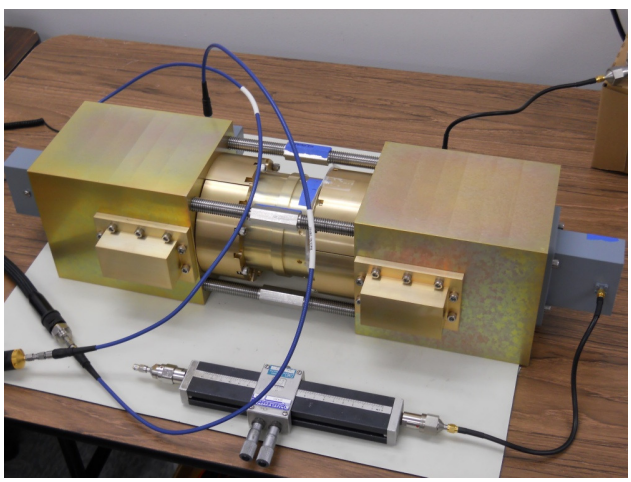

Figure 6: The power divider undergoing testing.

WAVEGUIDE COMPONENTS

For the installation at the Pegasus laboratory, we have acquired or built the major waveguide components, including a high-power phase shifter, directional coupler, power divider, and several adapters between different flange types. The power divider, shown in Figure 6, was designed and built by FAR-TECH using an idea developed at SLAC [7]. The device has four waveguide ports including an input port, an isolated port, and two output ports. In order to change the power split, the central cartridge must be freed by turning the four long threaded rods, allowing the cartridge to be rotated to the new setting. Adjustments to the power split are envisioned to occur infrequently, as adjusting the power would also de-pressurize of the SF_6-filled waveguide.

A challenge for the power divider RF design was to optimize the RF parameters (return loss, isolation, range of power split adjustment) while keeping the device as compact as possible, at just over 22 inches long. The device was optimized with a computer-based minimization procedure, which resulted in a measured isolation and return loss of better than 24 dB, and adjustment of the power split between 0% and >98% from the input to the axial output port that will be used for the linac, which will require about a 30% power split.

CONCLUSION

We have developed the conceptual design and much of the fabrication of a linac structure based on dual slot resonance coupling. Most of the large components for the waveguide power distribution system are also ready. Once completed, the linac will be tested at the UCLA Pegasus laboratory.

ACKNOWLEDGMENT

We thank R. Li, H. To, and P. Musumeci of UCLA for making preparations to test and incorporate the linac into their facility, including a CAD model of the waveguide layout, and particle tracking studies.

REFERENCES

[1] D. Newsham, N. Barov, R.H. Miller, Proc. of the 2011 Particle Accelerator Conference, p. 1897, (2011).
[2] U.S. Patent application #61166983.
[3] HFSS Manual, v11.0, Ansoft Corp.
[4] C. Ng et al., "State of the Art in EM Field Computation", Proc. of the 2006 EPAC Conference, (2006).
[5] D. Yu et. al, "A Plane-Wave-Transformer Photoelectron Linac", Proc. of the 1997 Particle Accelerators Conference, (1998).
[6] P. Musumeci, M.S. Butierrez, J.T. Moody, C.M. Scoby, "Time Resolved Relativistic Electron Diffraction", Proc. of the 2009 Particle Accelerators Conference, (2009).
[7] C.D. Nantista et al., "An RF Waveguide Distribution System for the ILC Test Accelerator at Fermilab's NML", Proc. 2007 Particle Accelerators Conference (2007).

Copyright © 2012 by IEEE – cc Creative Commons Attribution 3.0 (CC BY 3.0) — cc Creative Commons Attribution 3.0 (CC BY 3.0)

ISBN 978-3-95450-115-1